

## ORIGINAL ARTICLE

## Cracks in dentin and enamel after cryopreservation

Sebastian Kühl, DMD,<sup>a</sup> Hans Deyhle, PhD,<sup>b</sup> Melanie Zimmerli, DMD,<sup>a</sup> Giulio Spagnoli, PhD, MD,<sup>c</sup> Felix Beckmann, PhD,<sup>d</sup> Bert Müller, PhD,<sup>b</sup> and Andreas Filippi, MD, PhD, <sup>a</sup>Basel, Switzerland, and Hamburg, Germany

UNIVERSITY OF BASEL AND INSTITUTE OF MATERIALS RESEARCH

**Objective.** The objective of this study was to investigate if cryopreservation of teeth for long-term storage leads to cracks in enamel and dentin.

**Study Design.** Three teeth, which were extracted for orthodontic reasons, were cryopreserved in liquid nitrogen (temperature  $-196^{\circ}\text{C}$ ) and thawed according to standard protocols after 4 months. Micro computed tomography using synchrotron radiation was performed to detect cracks in the tooth hard tissues.

**Results.** Cracks were found in the enamel of all teeth, which are associated with forceps application during extraction. Cracks with a width larger than  $0.8\ \mu\text{m}$  were not identified in dentin and cementum.

**Conclusion.** Although cryopreservation of teeth according to the standard protocol does not generate cracks more than  $0.8\ \mu\text{m}$  wide, the use of forceps can result in prominent cracks. (Oral Surg Oral Med Oral Pathol Oral Radiol 2012;113:e5-e10)

One major requisite for the success of tooth replantation or transplantation is the survival of the periodontal cells (PDL) during extraoral tooth storage. Special cell nutrient media are available in which the periodontal cells can survive for about 24 hours and can be successfully used to store teeth after avulsion.<sup>1</sup>

In some indications, such as the extraction of healthy teeth for orthodontic reasons or tooth avulsion with extended damage of hard and soft tissues enabling an immediate replantation and transplantation, long-term storage of the extracted teeth (weeks up to years) is desirable.<sup>2</sup> Long-term storage of tissues and cells, without the loss of biological activity, can be successfully achieved by cryopreservation.<sup>2,3</sup> When cells are cooled under controlled conditions at temperatures lower than  $-130^{\circ}\text{C}$ , the biological time can effectively be stopped.<sup>4</sup> Cryopreservation of tissues for transplantation is generally performed at temperatures lower than  $-196^{\circ}\text{C}$ , because chemical reaction rates are massively elongated. At these temperatures, intracellular crystallization can occur, which is associated with the mechanical expansion of the intra-

cellular liquid. To avoid intracellular ice crystallite formation with consecutive irreversible cell damage, cryoprotective agents, such as dimethyl sulfoxide or glycerol, which have shown to successfully avoid this incidence, are applied. The sufficient penetration of the pulp soft tissue by cryoprotective agents represents a major problem during cryopreservation, as the apical foramen is often too small to guarantee a sufficient inflow. Schwarz<sup>5</sup> proved in the 1980s that, in contrast to PDL, the cells in the pulp do not survive cryopreservation because of insufficient penetration of cryoprotective agent and subsequent intracellular crystallization. The expansion of the pulp tissue might directly cause irreversible cracks in the hard tissues, having a negative impact on the prognosis of cryopreserved teeth used for transplantation. It is unknown whether cryopreservation causes cracks in dentin and enamel, as the proof is technically challenging. Histologic methods provide only 2-dimensional (2D) information; the sample preparation may result in a significant alteration or destruction of the 3-dimensional (3D) integrity of the specimen and as a result of sawing and grinding procedures a considerable part of the sample is lost and therefore inaccessible for evaluation.<sup>6</sup> The identification of cryopreservation-induced cracks is difficult owing to the preparation artifacts. Modern sawing and grinding techniques may avoid additional fractures but are extremely time-consuming and allow only 2D evaluation. Therefore, nondestructive and 3D imaging methods are needed. Micro computed tomography ( $\mu\text{CT}$ ) allows for the nondestructive visualization of hard tissues and therefore also for the cracks formed after treatments, such as cryopreservation. Synchrotron radiation-based  $\mu\text{CT}$  (SR $\mu\text{CT}$ ) takes advantage of highly intense, monochro-

<sup>a</sup>School of Dental Medicine, Department of Oral Surgery, Oral Radiology and Oral Medicine, University of Basel, Basel, Switzerland.

<sup>b</sup>Biomaterials Science Center, University of Basel, Basel, Switzerland.

<sup>c</sup>Institute for Surgical Research and Hospital Management and Department of Biomedicine, University of Basel, Basel, Switzerland.

<sup>d</sup>Institute of Materials Research, Helmholtz-Zentrum Geesthacht, Hamburg, Germany.

Received for publication May 25, 2011; returned for revision Jun 13, 2011; accepted for publication Jun 23, 2011.

© 2012 Elsevier Inc. All rights reserved.

2212-4403/\$ - see front matter

doi:10.1016/j.tripleo.2011.06.020

matic x-rays and, therefore, yields much better contrast than conventional laboratory-based x-ray sources. Consequently, cracks smaller than the voxel size cannot only be made visible, but using the mean absorption values within the crack area, one may deduce the average crack width with subvoxel precision. This estimate gives a lower limit for the detectable cracks of submicrometer width.

## MATERIAL AND METHODS

One incisor (12) and 2 unfilled premolars (14 and 24), termed tooth A, tooth B, and tooth C, were extracted for orthodontic reasons from a 21-year-old female patient and included in this investigation.

The teeth were removed under local anesthesia using a forceps at balanced forces. For the extraction of tooth A, the necessary forces were higher than for tooth B and tooth C. A detailed value, however, cannot be given. Immediately after extraction, the teeth were immersed in cell nutrition medium (Dentosafe; Dentosafe, GmbH, Iserlohn, Germany).

The teeth were cryopreserved within 2 hours after extraction. The teeth were removed from the cell nutrition medium (Dentosafe box) and transferred into Petri dishes filled with phosphate-buffered saline (PBS). To wash out blood and proteins adjacent to the tooth surfaces, the Petri dishes were gently agitated for several seconds manually. This procedure was repeated 3 times per tooth. Then, the teeth were transferred into special cryo-containers, filled with an optimized cell nutrition medium, including 50% RPMI 1640 medium (Invitrogen, Basel, Switzerland), 40% fetal-calf serum (FCS; Invitrogen), and 10% cryoprotective agent in form of dimethyl sulfoxide (DMSO, SIGMA, St. Louis, MO). The cryo-containers were sealed by a screw cap after immersing the teeth and stored in an isopropanol container at  $-70^{\circ}\text{C}$  for 12 hours for a slow and controlled freezing procedure. Subsequently, the cryo-containers were stored in the gas phase above liquid nitrogen ( $-196^{\circ}\text{C}$ ).

After a storage period of 4 months, the cryo-containers were removed from nitrogen tanks and transferred into a water bath with a temperature of  $37^{\circ}\text{C}$ . The specimens were kept under continuous agitation until the thawing process started. The teeth were subsequently removed from the cryo-containers and transferred to a Petri dish containing PBS to dilute and remove the cryoprotective agent. After 3 sessions of gentle agitation for 1 minute in PBS, the teeth were stored in a Dentosafe box for transport to the location of the synchrotron radiation source.

The SR $\mu$ CT-measurements were performed at the beamline W2 at HASYLAB (DESY, Hamburg, Germany), operated by the HZG Research Center in the standard absorption contrast tomography setup.<sup>7</sup> The

teeth were removed from the Dentosafe box and each tooth was transferred into a 1.5-mL Eppendorf tube filled with Dentosafe solution. The teeth were clamped into Eppendorf tubes based on their fitting size and shape. The specimen containers were glued onto the high-precision manipulator. Tooth A was measured at a photon energy of 36 keV with an asymmetric rotation axis.<sup>8</sup> There were 1440 projections acquired over  $360^{\circ}$  with a pixel size of  $2.8\ \mu\text{m}$ , resulting in a 3D dataset of  $2988 \times 2988 \times 1020$  isotropic voxels. Tooth B and tooth C were measured at a photon energy of 41 keV with an asymmetric rotation axis in 4 height steps each. The  $360^{\circ}$  scan with a pixel size of  $4.1\ \mu\text{m}$  generated a total of 1440 projections resulting in a dataset of  $2884 \times 2884 \times 4966$  and  $2940 \times 2940 \times 4940$  isotropic voxels, respectively. The data reconstruction was carried out by means of the filtered back-projection algorithm and with a binning factor of 2.<sup>9</sup>

The dataset of each tooth was converted into DICOM format to be visually analyzed. Two oral surgeons, experienced in the evaluation of 3D data, scrolled through the 3D data in x-, y-, and z-directions to detect the cracks. After this evaluation, each examiner described the cracks.

Selected cracks were further examined to determine their average width. First, a volume of interest was determined. The histogram of this region of interest was quantitatively evaluated by means of dedicated Matlab code (MATLAB, MathWorks, Natick, MA).

## RESULTS

The composition of hard tissues of teeth (dentin and enamel) are known and the related local x-ray absorption values allow segmenting dentin, enamel, and surrounding PBS, as qualitatively illustrated in Figures 1 to 3. Consequently, cracks with a width above specific thresholds become visible in the virtual cuts and 3D representations of the computed tomography (CT) data (see Figure 1).

Tooth A contained numerous characteristic features identified as cracks in the enamel. The CT slices in Figure 1 reveal discontinuities of the gray-scale-related x-ray absorption values within the enamel, identified as micrometer-wide cracks. The cracks are generally aligned perpendicular to the dentin-enamel junction and seem to stop at this internal interface. In the diagonally opposite periapical regions, a high density of cracks is present, as distinctly demonstrated by the 3D image to the right in Figure 1.

Figure 2 shows slices and 3D renderings of tooth B. Again, one can perfectly discriminate between enamel and dentin as well as surrounding PBS. The virtual cut along the tooth axis shows areas of reduced intensity, which originated from the stacking and can be regarded

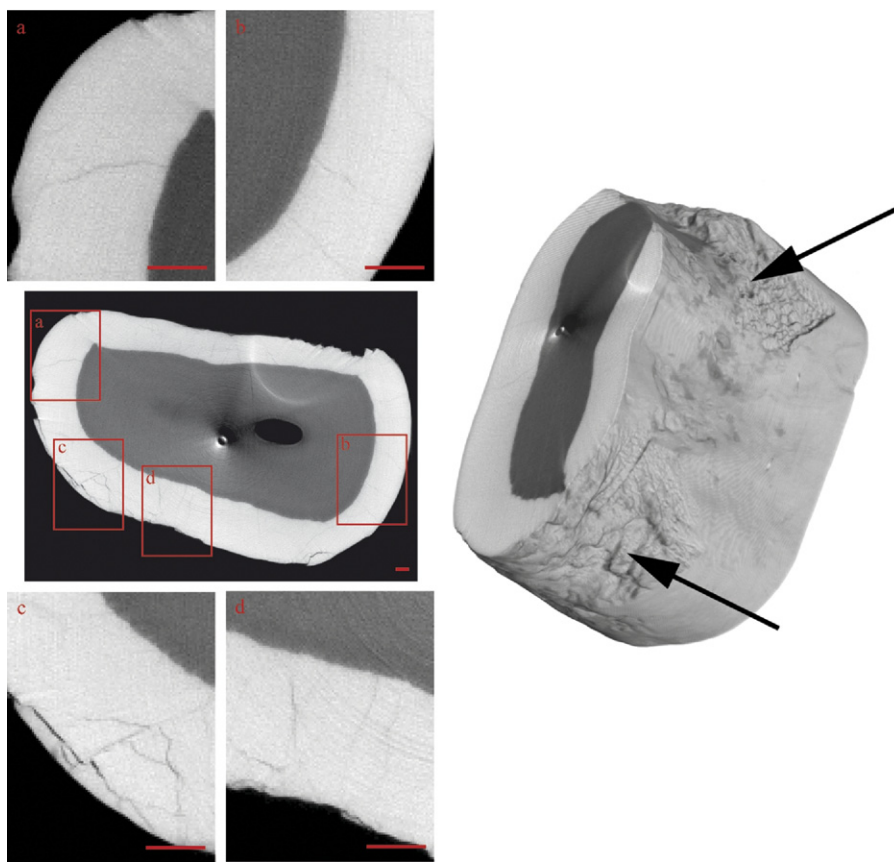


Fig. 1. On the left, the 5.6- $\mu\text{m}$  thin, horizontal slices through the 3D-data of Tooth A contain microstructures exhibiting the characteristic morphology and x-ray absorption of cracks. The related 3D rendering on the right indicates that the cracks are generated by the forceps used for tooth extraction. The scale bars correspond to 300  $\mu\text{m}$ .

as artifacts. There are a fewer number of cracks, however, than in tooth A. These cracks are visible only within the enamel and are almost perfectly perpendicular to the dentin-enamel junction.

The cracks within the enamel usually show higher local x-ray absorption values than the PBS, indicating partial volume phenomena. This means that the cracks are significantly thinner than the voxel length. Because the SR $\mu$ CT data of the hard tissues are quantities represented by strong contrast, the width of the crack can be reasonably estimated by means of the local x-ray absorption. To determine the precision of this approach, the histogram of the local x-ray absorption values, as represented by gray values in Figures 1 and 2, is analyzed and shown in Figure 3. The PBS and enamel peaks are well approximated by Gaussians.<sup>10</sup> The position of these Gaussians along the x-axis exhibits the mean x-ray absorption of PBS and enamel, whereas the half width relates to the photon statistics and variations of the x-ray density. For the PBS, a homogeneous medium, density variations can be excluded, which means that the full width at half maximum (FWHM) yields the density resolution or the maximal possible

contrast.<sup>11</sup> A crack can be identified if its presence reduces the local absorption coefficient by a value larger than the FWHM. The histogram of tooth B in Figure 4 shows the enamel peak at the x-ray absorption of 2.50  $\text{cm}^{-1}$  with an FWHM of 0.15  $\text{cm}^{-1}$  and the PBS peak at 0.24  $\text{cm}^{-1}$  with an FWHM of 0.10  $\text{cm}^{-1}$ . This means that cracks with a width of one-tenth voxel length can be quantitatively evaluated. The photon statistics, however, result in a noise level that does not permit the measurement of the width at each position. Reasonably large subvolumes, as indicated in Figure 4, however, enable us to measure the mean crack width within this region of interest, analyzing the histogram of the local x-ray absorption values. Figure 4 elucidates the procedure. First, only the right part of the enamel peak is fitted using a Gaussian, because the left one (toward lower x-ray absorption) is affected by the crack. Second, the difference between the measured histogram and the Gaussian fit yields the voxels of the crack. Third, the mean local x-ray absorption of these voxels ( $2.26 \pm 0.25 \text{ cm}^{-1}$ ) can be related to the difference between the average x-ray absorption of enamel and PBS. Consequently, the mean width of the crack(s)

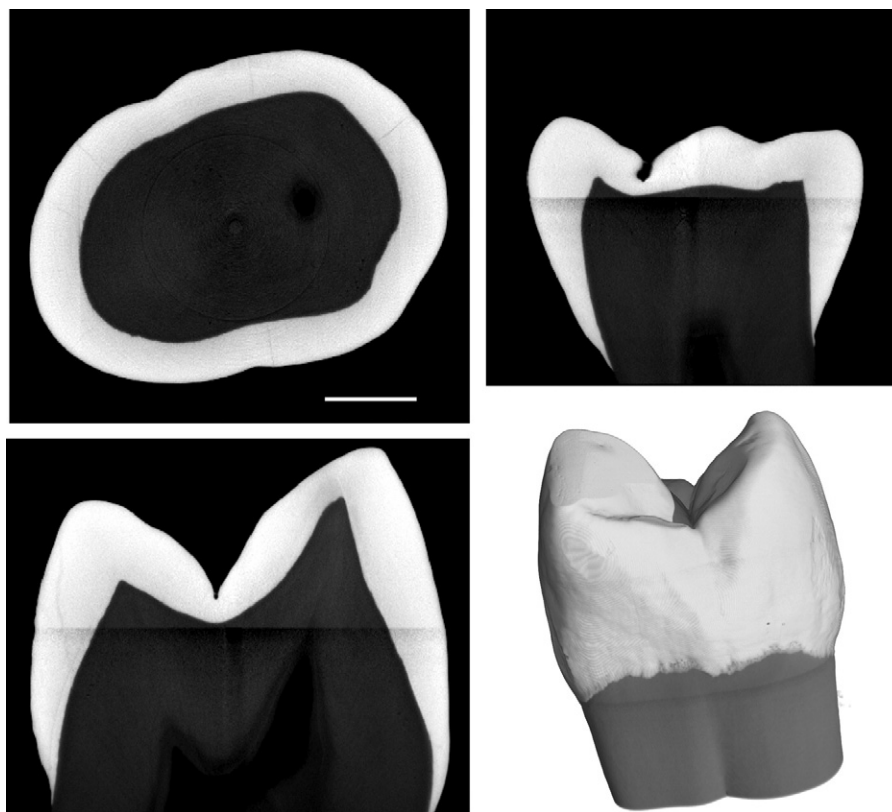


Fig. 2. The 3 orthogonal slices through Tooth B together with a 3D rendering show only a limited number of cracks oriented perpendicular to the dentin-enamel junction. One recognizes 3 height steps because of the reduced photon statistics in the transition regions. The length bar corresponds to 2 mm.

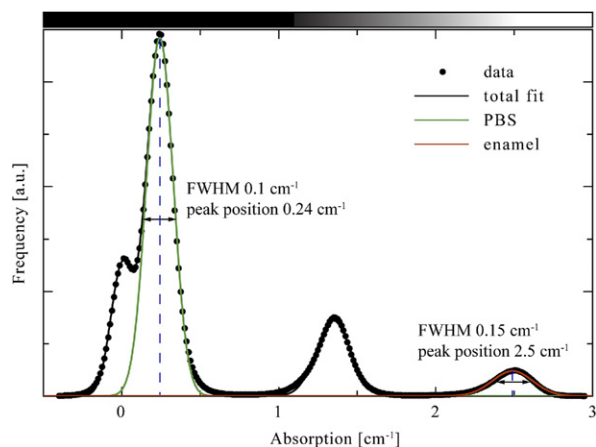


Fig. 3. Absorption histogram of the entire Tooth B. PBS (green-colored peak) and enamel (red colored) were fitted with Gaussians. In black, the total fit of the 4 components is given. The recolored fit exhibits an asymmetry with respect to the measured values, indicating a few cracks or other density inhomogeneities.

within the region of interest corresponds to less than one-tenth of the isotropic voxel length, namely to the average crack width of  $(0.71 \pm 0.19 \mu\text{m})$ .

### DISCUSSION

Schwarz<sup>5</sup> showed that periodontal cells can survive cryopreservation if the cooling has been performed in an appropriate manner. Oh et al.<sup>4</sup> observed 96% viability of PDL cells after cryopreservation. The cells in the pulp, however, were severely damaged during the cryopreservation, because the agent only insufficiently penetrated into the pulp cavity through the apical orifice of the root.<sup>12</sup> Intracellular crystallization increases not only the width of the cells in the pulp but also the size of the odontoblastic dendrites localized in the dentinal tubules. The expansion owing to the ice crystallization usually results in the formation of cracks in hard tissue. The question arises whether the crack formation can be suppressed or not. Therefore, SR $\mu$ CT was applied to investigate cryopreserved teeth for cracks after the thawing procedure according to the given protocols.<sup>4,12-16</sup> As the spatial resolution and the contrast of SR $\mu$ CT are limited, one can observe cracks with a width only above a certain threshold. In agreement with previous studies, the width of the cracks can be much smaller than the isotropic pixel length,<sup>16</sup> namely in the present case about one-tenth. This is a rather pessimistic estimate, as experienced dentists can identify cracks

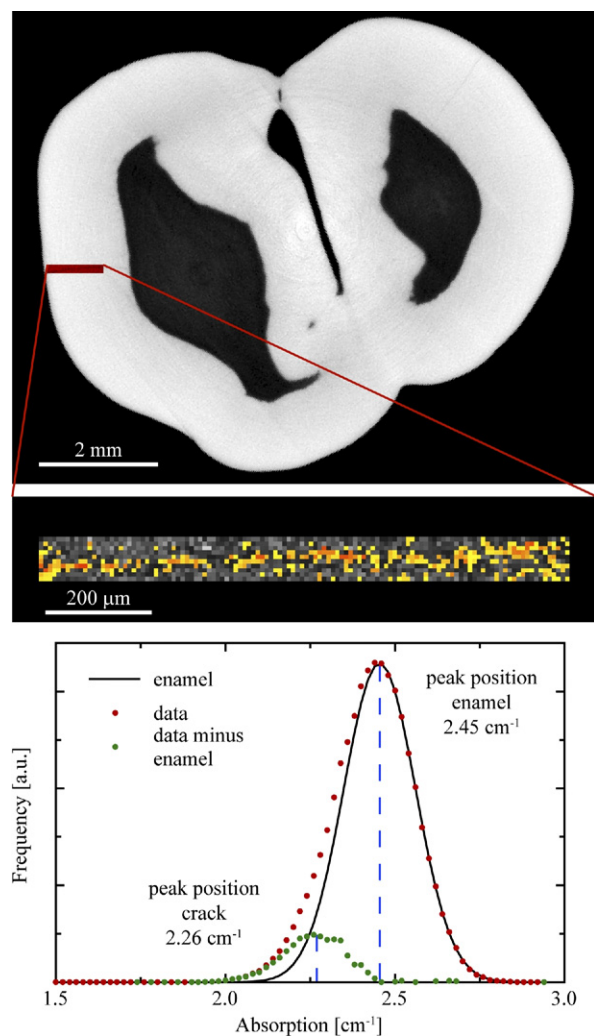


Fig. 4. A subvolume of  $1.97 \times 10^5$  voxels containing part of a crack is extracted from the dataset of Tooth B (red area in the topmost image). Magnification of a cut through the selected volume is shown in the center image. Because of noise, the crack (yellow-orange) cannot be unequivocally segmented from the sound enamel (gray). The diagram shows the histogram of the extracted volume, including data treatment.

with an even smaller width in our 3D datasets. In general, however, not only the width but also the morphology of the crack should be made visible. Here, the application of deformable contour models was shown to yield reasonable results.<sup>17</sup> The present study demonstrates that tooth B and tooth C (not shown) exhibit only a small number of micrometer-wide cracks in enamel and no such cracks in the dentin. This indicates that the freezing procedure has been already developed to a high level. It would probably have been advantageous to perform SR $\mu$ CT before and after cryopreservation and to compare the width and length of visible cracks. The location and course of the cracks, however, clearly show that they rather result from the applied

forces during extraction than from expansions during cryopreservation. Cryo-related cracks would probably have affected enamel and dentin. The numerous cracks of tooth A that were mostly generated during tooth extraction reveal the necessity to significantly improve the extraction procedure, maybe by using a force-controlled forceps, which better distributes the applied force onto the tooth surface. On enamel fracture, Sognnaes<sup>18</sup> showed that teeth that have been in use are often riddled with enamel lamellae (cracks), even in the young. These cracks probably start from tufts from inside to outside.<sup>19</sup> The cracks in our study begin at the dentin-enamel junction, where the forceps was applied. It has been suggested that enamel is actually designed to crack in ways that prevent loss of tooth function.<sup>20</sup> The forceps application may have opened preexisting cracks. However, the perpendicular alignment of the cracks seems not to be related to cryopreservation but is the result of mechanical forces from the forceps. Cracks in the dentin should have a higher clinical impact than in enamel, because the enamel leakages affect only the coronal part of teeth. As after cryopreservation, endodontic treatment is inevitable,<sup>13</sup> leakages in enamel are not the focus of treatments. Leakages in the dentin, however, might have a significant impact on transplanted teeth, as the leakages are localized in the bony level of teeth affecting the periodontal tissues. It is well known that such leakages may cause chronic inflammation with consecutive bone loss. Especially in transplanted teeth, where higher regenerative capacities of the periodontal tissues are required, cracks probably have even more negative long-term effects.

The sample size of reviewed teeth is rather low. This weakens the general statement on the formation of cracks after cryopreservation. Nevertheless, the results of the present study indicate that the risk of crack formation owing to the applied forces for tooth removal is significantly higher than as the result of cryopreservation. Fortunately, no crack was found within the dentin. As the threshold for the cracks in the dentin can be estimated to be between one-fourth and one-fifth of the pixel length, we conclude that the cracks in dentin are absent or smaller than 1.84- $\mu$ m wide. Cryopreservation as performed may lead to only a very few cracks in the enamel, whereas inappropriate tooth removal can generate numerous cracks. Future studies with a higher number of examined teeth and a direct comparison of high-resolution SR $\mu$ CT at 2 different stages (before and after cryopreservation) are needed to confirm the findings of this study.

#### REFERENCES

1. Pohl Y, Filippi A, Kirschner H. Results after replantation of avulsed permanent teeth. II. Periodontal healing and the role of

- physiologic storage and antiresorptive-regenerative therapy. *Dent Traumatol* 2005;21:93-101.
2. Zimmerli M, Filippi A. [Cryopreservation of teeth]. *Schweiz Monatsschr Zahnmed* 2010;120:423-34.
  3. Mazur P. Freezing of living cells: mechanisms and implications. *Am J Physiol* 1984;247:125-42.
  4. Oh YH, Che ZM, Hong JC, Lee EJ, Lee SJ, Kim J. Cryopreservation of human teeth for future organization of a tooth-bank—a preliminary study. *Cryobiology* 2005;51:322-29.
  5. Schwarz O. Cryopreservation of teeth before replantation. In: Andreasen J, editor. *Atlas of replantation and transplantation of teeth*. Fribourg: Mediglobe; 1982. p. 242-56.
  6. Nagasawa S, Yoshida T, Tamura K, Yamazoe M, Hayano K, Arai Y, et al. Construction of database for three-dimensional human tooth models and its ability for education and research—cariouss tooth models. *Dent Mater J* 2010;29:132-7.
  7. Beckmann F, Herzen J, Haibel A, Müller B, Schreyer A. High density resolution in synchrotron-radiation-based attenuation-contrast microtomography. *Proc SPIE* 2008;7078:70781D.
  8. Müller B, Bernhardt R, Weitkamp T, Beckmann F, Bräuer R, Schurigt U, et al. Morphology of bony tissues and implants uncovered by high-resolution tomographic imaging. *Int J Mater Res* 2007;98:613-21.
  9. Kak AC, Slaney M. Principles of computerized tomographic imaging. New York: IEEE Publications; 1988. p. 99-107.
  10. Müller B, Beckmann F, Huser M, Maspero F, Székely G, Ruffieux K, et al. Non-destructive three-dimensional evaluation of a polymer sponge by micro-tomography using synchrotron radiation. *Biomol Eng* 2002;19:73-8.
  11. Thurner P, Beckmann F, Müller B. An optimization procedure for spatial and density resolution in hard x-ray micro-computed tomography. *Nuc Instr Meth Physiol Res* 2004;225:599-603.
  12. Price PJ, Cserepfalvi M. Pulp vitality and the homotransplantation of frozen teeth. *J Dent Res* 1972;51:39-43.
  13. Kawasaki N, Hamamoto Y, Nakajima T, Irie K, Ozawa H. Periodontal regeneration of transplanted rat molars after cryopreservation. *Arch Oral Biol* 2004;49:59-69.
  14. Schwartz O. Cryopreservation as long-term storage of teeth for transplantation or replantation. *Int J Oral Maxillofac Surg* 1986;15:30-2.
  15. Schwartz O, Andreasen JO, Greve T. Cryopreservation of mature teeth before replantation in monkeys; II. Effect of preincubation, different freezing rates and equilibration times and root canal treatment. *Int J Oral Surg* 1983;12:425-36.
  16. Breunig TM, Stock SR, Guvenilir A, Elliott JC, Anderson P, Davis GR. Damage in aligned-fibre sic/al quantified using a laboratory x-ray tomographic microscope. *Composites* 1993;24:209-13.
  17. Müller B, Pfrunder F, Chiocca L, Ruse ND, Beckmann F. Visualising complex morphology of fatigue cracks in voxel based 3D datasets. *Mater Sci Technol* 2006;22:1038-44.
  18. Sognaes RF. The organic elements of the enamel; the gross morphology and the histological relationship of the lamellae to the organic framework of the enamel. *J Dent Res* 1950;29:260-9.
  19. Chai H, Lee JJ, Lawn BR. Fracture of tooth enamel from incipient microstructural defects. *J Mech Behav Biomed Mater* 2010;3:116-20.
  20. Chai H, Lee JJ, Constantino PJ, Lucas PW, Lawn BR. Remarkable resilience of teeth. *Proc Natl Acad Sci U S A* 2009; 106:7289-93.
- Reprint requests:*  
Sebastian Kühl, DMD  
School of Dental Medicine  
Department of Oral Surgery, Oral Radiology and Oral Medicine  
University of Basel  
Hebelstrasse 3  
4056 Basel, Switzerland  
Sebastian.kuehl@unibas.ch